ACDIV-2014-08
September, 2014

OVERVIEW OF THE GEOMETRICAL NON-LINEAR EFFECTS OF BUTTON BPMS AND METHODOLOGY FOR THEIR EFFICIENT SUPPRESSION

A. A. Nosych, U. Iriso, A. Olmos, ALBA CELLS, Barcelona, Spain
M. Wendt, CERN, Geneva, Switzerland

Abstract:

This paper describes an overview of the geometric nonlinear effects common to beam position monitors (BPMs) installed in the accelerators and a methodology to correct for these effects. A typical characteristic curve of a pick-up is linear within a limited range from the BPM origin. At larger offsets the non-linearity of the curve is more pronounced and gets worse if the button diameter is small with respect to the beam pipe diameter. The general real-time linearization methods usually utilize linear correction combined with a simplistic polynomial, which may lead to inaccuracies in their limited application. We have developed a more rigorous methodology to suppress the non-linear effects of the BPMs through electromagnetic (EM) simulations and 2D fitting approximations. The focus is mainly on standard button pickups for the electron (ALBA) and proton machines (LHC).

Accelerator Division
Alba Synchrotron Light Source
Ctra. BP 1413 Km. 3,3
08290 Cerdanyola del Valles, Spain

OVERVIEW OF THE GEOMETRICAL NON-LINEAR EFFECTS OF BUTTON BPMS AND METHODOLOGY FOR THEIR EFFICIENT SUPPRESSION

A. A. Nosych, U. Iriso, A. Olmos, ALBA CELLS, Barcelona, Spain
M. Wendt, CERN, Geneva, Switzerland

Abstract

This paper describes an overview of the geometric non-linear effects common to beam position monitors (BPMs) installed in the accelerators and a methodology to correct for these effects. A typical characteristic curve of a pick-up is linear within a limited range from the BPM origin. At larger offsets the non-linearity of the curve is more pronounced and gets worse if the button diameter is small with respect to the beam pipe diameter. The general real-time linearization methods usually utilize linear correction combined with a simplistic polynomial, which may lead to inaccuracies in their limited application. We have developed a more rigorous methodology to suppress the non-linear effects of the BPMs through electromagnetic (EM) simulations and 2D fitting approximations. The focus is mainly on standard button pick-ups for the electron (ALBA) and proton machines (LHC).

INTRODUCTION

BPMs are among the most important and numerous parts of a diagnostics system of any particle accelerator. Accelerators require constant beam orbit monitoring in order to control the quality of passing beams and allow various feedback systems to improve it. Usually beams travel close to geometrical centers of BPMs on their way, following the optimal "golden" orbit. However, beams are sometimes intentionally steered away from the optimal orbit, whether it is to increase the crossing angle in order to improve luminosity of a collider (LHC), or to study the non-linear magnetic field components of a storage ring (ALBA).

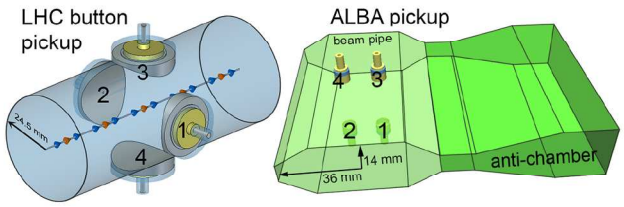

Figure 1: 3D models of a typical LHC curved-button pickup and a standard pickup of ALBA.

Every beam position reading of a BPM is subject to non-linear errors. The non-linear behavior of a BPM pickup is caused by its geometrical design and the resulting errors are more pronounced at larger beam offsets from the BPM origin. In this paper we will describe two standard BPM geometries, one belonging to LHC: a proton collider, and another to ALBA: a synchrotron light source (both geometries are shown in Fig. 1). After discussing the modeling and simulation process we will summarize non-linear effects of the BPMs' characteristic response for different signal treatments, and address results of an efficient non-linearity correction using high-order surface (2D) polynomials.

MODELLING AND MAPPING A BPM

Left in Fig. 1 is a common 4-button (arranged 90^o apart) pickup mounted on a beam pipe of circular cross-section (radius $R_{\text{lhc}} = 24.5$ mm) belonging to the LHC. Right in Fig. 1 is a flat-button BPM used in ALBA, a 3 GeV synchrotron light source, with 2 pairs of buttons located above and below the beam, which travels in a hexagonal beam pipe of 72×28 mm transversely ($R_{\text{alba}} = 36$ mm).

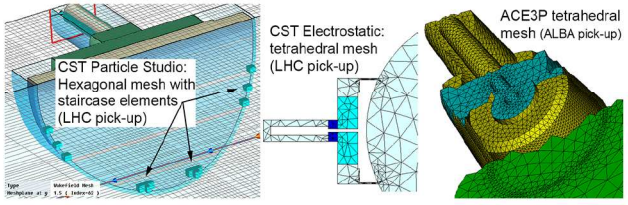

Figure 2: Meshing BPM buttons with hexahedral mesh of CST Particle Studio and tetrahedral meshes of CST Electrostatic and ACE3P.

As usual in light sources, parts of ALBA vacuum chamber include the anti-chamber used for photons. Depending on location in the storage ring, the anti-chamber has different dimensions; one of them is shown in Fig. 1 right. Here the beam pipe loses its symmetry in Y plane; however, we have studied 2 types of anti-chambers attached to the same BPM module, and have not observed any noticeable effect on BPM sensitivity. Hence, in our studies we consider all types of ALBA beam pipes symmetric, omitting the anti-chamber.

To simulate BPM response of the LHC button in time-domain we have initially used CST Particle Studio [1]. We have found that for 3D geometry with small curved elements (e.g. a curved button and a curved vacuum gap around it, Fig. 2 left) the hexahedral mesh of CST PS is not very efficient: in pursuit to approximate curves by orthogonal edges, the mesh cells greatly multiply in numbers (at least 6M mesh cells for this BPM), leading to lengthy simulations: it took 25 minutes on a desktop PC with 2x3.5 GHz CPU and 8 Gb RAM to simulate a single beam transit.

To avoid this time waste we have switched to the Electrostatic solver of CST in "semi-2D" mode [2], using the tetrahedral mesh with more accurate approximation of curved elements. The solver itself does not allow a true 2D input, so we introduce a 1 mm thick "slice" of the BPM with magnetic

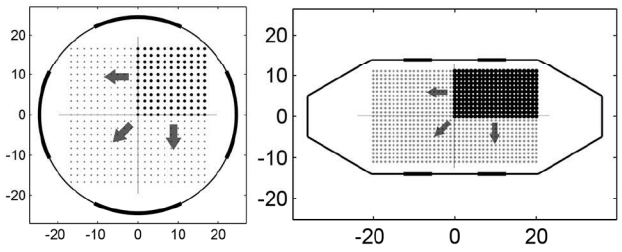

Figure 3: Mapping layout of LHC (left) and ALBA (right) BPMs with equidistant grid covering the first quadrant of the coordinate system.

boundaries at the z-planes (Fig. 2 middle). The electrostatic potentials are then evaluated for one BPM electrode and, due to symmetries, restored for others by mirroring/rotation. The obtained potentials are then combined for the normalized horizontal/vertical potential, which is equivalent to the normalized line charge (the beam) position. A single simulation maps the entire BPM in seconds.

To simulate the ALBA pick-up we have used the 3D time-domain solver (T3P) of ACE3P [3], which also offers tetrahedral meshing (Fig. 2 right) and quick (within minutes) simulations on parallel CPU clusters. The BPM was excited with a single relativistic bunch excitation (Q=3.4E-10 C, σ_τ=5 mm). To simulate the BPM response as a function of beam position, a beam displacement parameter sweep within a quadrant in the transverse plane (as shown in Fig. 3) was executed in T3P using the transverse beam coordinates (x, y) as iteration parameters with constant step size. At each beam position the peak voltage $V_{i=1,2,3,4}$ of every BPM port was logged. Due to 4-fold symmetry of the ALBA BPM, the mapped quarter-grid is then mirrored (taking into account appropriate sign swaps) to reproduce a full map, thus describing behavior of the entire BPM. We have stayed with a 41×23 grid ($\pm 20 \times \pm 11$ mm) for the ALBA BPM, and a 21×21 grid ($\pm 17 \times \pm 17$ mm) for the LHC pickup. The initial choice of grid size, step size and number of grid points is open; however, it has an impact on the quality of beam position linearization and area of efficient correction.

We consider the 3D approach as the default technique, as it accurately takes all beam-induced effects (e.g. resonances, non-TEM effects, etc.) into account. Analysis of the mentioned tools for BPM modelling was previously discussed in [2] in more detail.

NON-LINEARITY TREATMENT

By comparing the signals of opposite sets of electrodes, a beam intensity independent, normalized beam position signal can be deduced. There are several ways to restore the beam position from 4-button BPM signals due to distinct button arrangements in considered geometries. We will show three examples of common linear signal treatments.

Difference over Sum

In a simplistic symmetric BPM button arrangement around a circular vacuum chamber (LHC case), the pickup response can be approximated by a wall-current model, where the normalized position characteristic in the XY plane is described in general by

$$x^{\mathrm{lhc}}_{\mathrm{dos}} = k_x \times \frac{V_1 - V_2}{V_1 + V_2}\ , \quad y^{\mathrm{lhc}}_{\mathrm{dos}} = k_y \times \frac{V_3 - V_4}{V_3 + V_4} \qquad (1)$$

Here k_x, k_y are the linear calibration constants to mm, and in fact, for circular beam pipes they are approximated by $k_{x,y} = R/2$ [2]. Equation 1 represents a classic linear approach, usually referenced as the Difference Over Sum (DOS), its application is plotted in Fig. 4 for horizontal sweeps at fixed vertical offsets and for a full mapped grid of the LHC BPM. Here the linear region of $k_{x,y}$ is within $x, y = \pm 7$ mm.

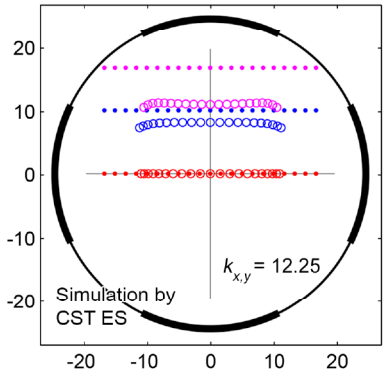

(a) Horizontal beam sweeps for 3 vertical displacements.

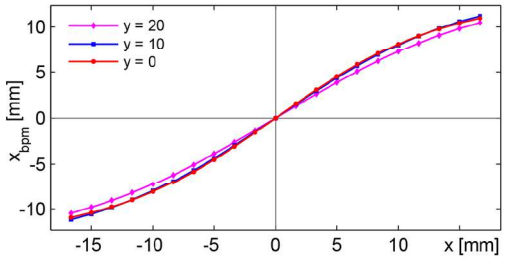

(b) Characteristic curves of the beam sweeps above.

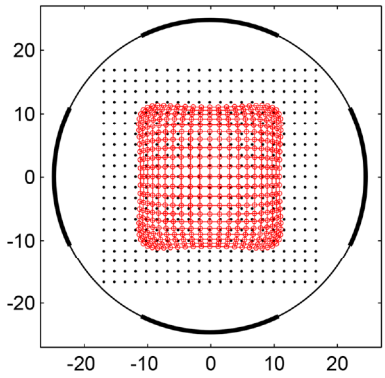

(c) Mapped grid of $(x^{\mathrm{lhc}}_{\mathrm{dos}}, y^{\mathrm{lhc}}_{\mathrm{dos}})$.

Figure 4: Results of DOS application to LHC BPM map.

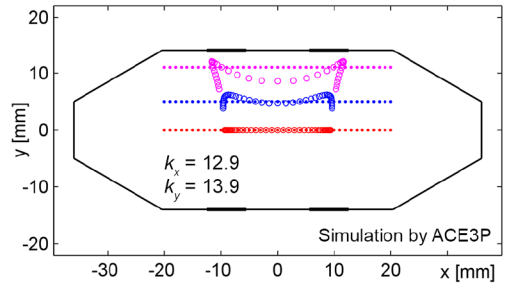

(a) Horizontal beam sweeps for 3 vertical displacements.

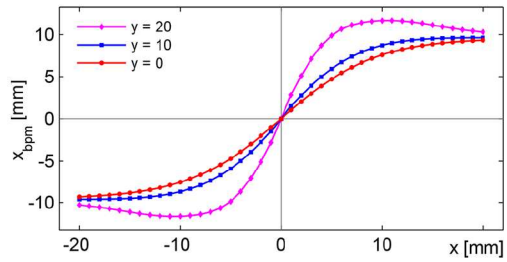

(b) Characteristic curves of the beam sweeps above.

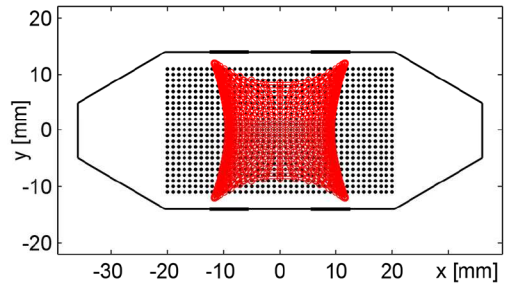

(c) Mapped grid of $(x^{\text{alba}}_{\text{dos}}, y^{\text{alba}}_{\text{dos}})$.

Figure 5: Results of DOS application to ALBA BPM map. Anti-chamber is not shown.

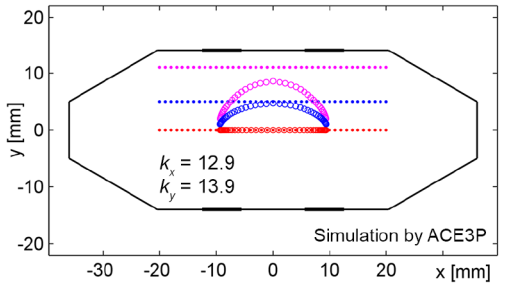

(a) Horizontal beam sweeps for 3 vertical displacements.

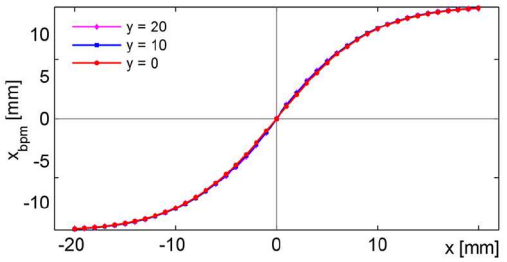

(b) Characteristic curves of the beam sweeps above.

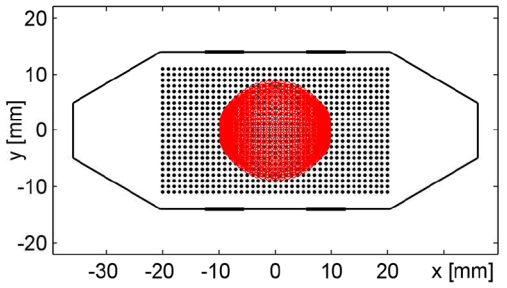

(c) Mapped grid of $(x^{\text{alba}}_{\text{diag}}, y^{\text{alba}}_{\text{diag}})$.

Figure 6: Diagonal treatment of ALBA BPM map.

Due to button placement in the ALBA BPM, a modification of DOS is used to normalize the electrode signals [4]:

$$x^{\text{alba}}_{\text{dos}} = k_x \times \frac{V_3 + V_1 - V_4 - V_2}{V_1 + V_2 + V_3 + V_4} \tag{2}$$

$$y^{\text{alba}}_{\text{dos}} = k_y \times \frac{V_3 + V_4 - V_2 - V_1}{V_1 + V_2 + V_3 + V_4} \tag{3}$$

Here $k_{x,y}$ can be approximated by the slope of the characteristic curve (linear part of it) for each axis separately, e.g. the red curve ($y = 0$) for $|x| \leq 5$ mm in Fig. 5(b) can provide a corresponding constant k_x. However, this approach has limited application due to strong cross-coupling between X and Y offsets and non-linear behavior of k_x and k_y already for arbitrary beam offsets.

Diagonal Treatment

By using a so-called "diagonal" treatment [5, 6] of the ALBA BPM signals

$$x^{\text{alba}}_{\text{diag}} = \frac{k_x}{2} \times \left[\frac{V_3 - V_2}{V_3 + V_2} - \frac{V_4 - V_1}{V_4 + V_1}\right] \tag{4}$$

$$y^{\text{alba}}_{\text{diag}} = \frac{k_y}{2} \times \left[\frac{V_3 - V_2}{V_3 + V_2} + \frac{V_4 - V_1}{V_4 + V_1}\right] \tag{5}$$

a much smaller coupling within the central part of the BPM is obtained. A pair of constant calibration factors $k_{x,y}$ can provide linearization for an arbitrary beam offset within $x, y = \pm 5$ mm, as can be observed in Fig. 6(b): for three different beam sweeps the characteristic curves are almost identical. Compared to previous DOS treatment, the diagonal approach is favorable for BPMs where the buttons are not located along the transverse axis, and beams stay within the close vicinity of beam pipe center.

POLYNOMIAL CORRECTION

Linear analysis demonstrates that no electrode configuration of a button BPM can supply a perfect linear beam position response. Their position sensitivity is not only non-linear, particular for large beam displacements, but the maps

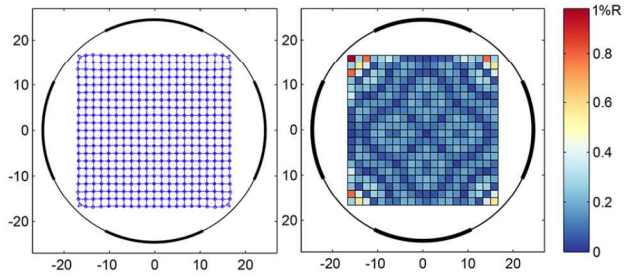

Figure 7: 9th-order polynomial correction of LHC BPM grid $(x^{\mathrm{lhc}}_{\mathrm{dos}}, y^{\mathrm{lhc}}_{\mathrm{dos}})$ (right), and its error map (left).

in Figs. 4(c)-6(c) also show a "pin-cushion" effect, indicating cross-coupling between XY planes. In a general case of an arbitrary BPM cross-section, the position characteristic of the pickup cannot be approximated by a closed analytical form, and therefore must be evaluated in a different way.

Based on the studies done in [2,7] for LHC stripline BPMs, we have applied the polynomial fitting technique to both considered pickups. Applying a mapping scheme, a pair of polynomial functions (one per each plane) of the following form allows to adequately compensate non-linearity of the BPM response within the considered mapped grid, taking into account the cross-coupling:

$$F^{\mathrm{x,y}}_{pq}(x_{bpm}, y_{bpm}) = \sum_{i,j=0}^{p,q} C^{\mathrm{x,y}}_{ij} x^i_{bpm} y^j_{bpm} \qquad (6)$$

Here $C^{\mathrm{x,y}}_{ij}$ is a set of calculated coefficients per each corresponding plane X and Y, p and q are maximum powers of each variable, and (x_{bpm}, y_{bpm}) are the uncorrected sets of beam position values, i.e. $(x^{\mathrm{lhc}}_{\mathrm{dos}}, y^{\mathrm{lhc}}_{\mathrm{dos}})$, $(x^{\mathrm{alba}}_{\mathrm{dos}}, y^{\mathrm{alba}}_{\mathrm{dos}})$ or $(x^{\mathrm{alba}}_{\mathrm{diag}}, y^{\mathrm{alba}}_{\mathrm{diag}})$. We have determined that already low-power polynomials provide sufficient quality of correction. For brevity, here we will focus only on the 9th-order polynomials.

An absolute error map is defined as distances (in mm) between initial beam positions and corrected positions by the polynomial. For convenience, it is displayed as color-coded map with error values normalized to the aperture R, such that all error values above 1% of R are colored in red.

Figure 7 shows application of the calculated polynomial to the LHC BPM grid: the corrected map and its 2D error. Here, an overall quality of correction is well below 75 μm (0.3% of R_{lhc}) except the grid corners, where the beam is unlikely to drift.

Partial Correction

In any accelerator the beam is typically allowed to circulate within limited offsets from the beam pipe center. Larger drift will be detected by interlock BPMs and the beam will be automatically dumped. For the first study on ALBA BPM, consider the "beam allowed" limit as 21×23 points ($\pm 10 \times \pm 11$ mm) - a subset of previously defined grid. By including the limited grids of both DOS (Eq. 2) and diagonal (Eq. 4) normalization types in the polynomial routine, we calculate 9th-order polynomials which are efficient only in the "allowed" area. Figures 8(a,b) and Figures 9(a,b) show a zoom into the corrected maps and errors after applying these polynomials corresponding to DOS or diagonal-type grids. Here blue points belong to the "beam allowed" area, included in the polynomial fits, while red ones were ini-

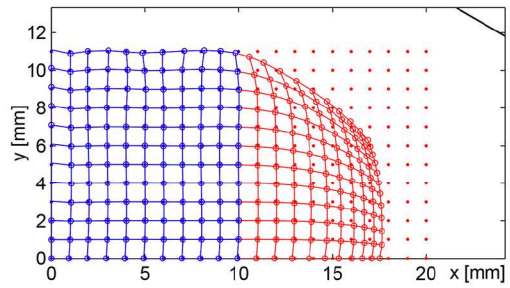

(a) Corrected grid of $(x^{\mathrm{alba}}_{\mathrm{dos}}, y^{\mathrm{alba}}_{\mathrm{dos}})$ (zoom),

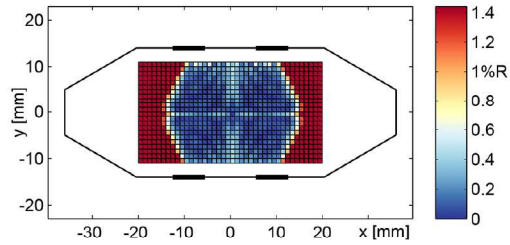

(b) and its error map.

Figure 8: 9th-order polynomial correction of partial ALBA BPM grid after DOS signal treatment.

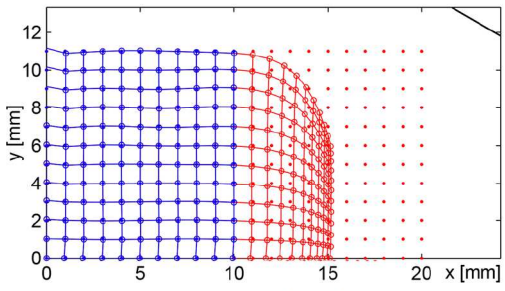

(a) Corrected grid of $(x^{\mathrm{alba}}_{\mathrm{diag}}, y^{\mathrm{alba}}_{\mathrm{diag}})$ (zoom),

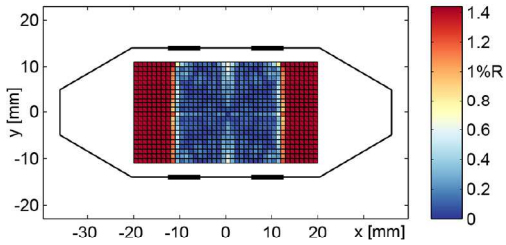

(b) and its error map.

Figure 9: 9th-order polynomial correction of partial ALBA BPM grid after diagonal signal treatment.

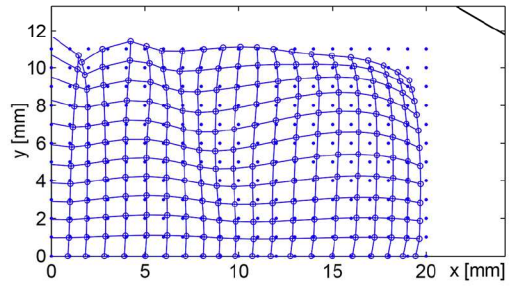

(a) Corrected grid of $(x^{\text{alba}}_{\text{dos}}, y^{\text{alba}}_{\text{dos}})$ (zoom),

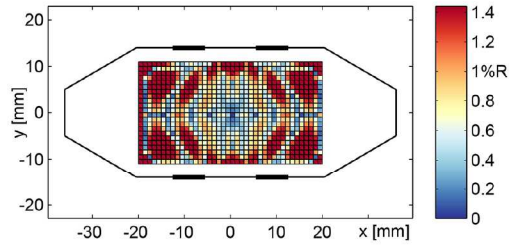

(b) and its error map.

Figure 10: 9th-order polynomial correction of a full ALBA BPM grid after DOS normalization.

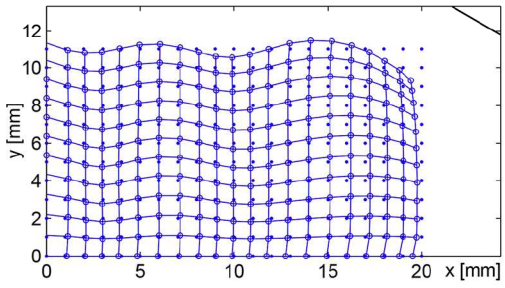

(a) Corrected grid of $(x^{\text{alba}}_{\text{diag}}, y^{\text{alba}}_{\text{diag}})$ (zoom),

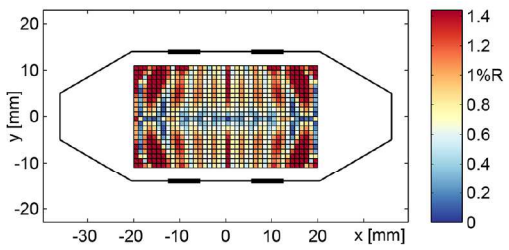

(b) and its error map.

Figure 11: 9th-order polynomial correction of a full ALBA BPM grid after diagonal normalization.

tially excluded. The overall correction efficiency for both normalization types is under 200 μm (0.6 % of R_{alba}).

Complete Correction

Limiting the BPM map can be useful to gain linearization accuracy in the central area of a BPM, when the correction beyond is not important. Larger-scale correction can be done by deriving a polynomial based on the maximal mapped grid of points. Results of such approach (also for 9th-order polys) are shown in Figs. 10 and 11 for both normalization types of ALBA BPM.

There is a clear reduction of accuracy seen in both error maps, especially along the axes in Figs. 10(b) and 11(b). To avoid this one could increase the polynomial powers, possibly, at the cost of some processing speed on the fly. We consider testing it in the future.

CONCLUSIONS AND OUTLOOK

In this work we analyzed several types of geometrical non-linear effects which deteriorate the BPM response of two standard BPM pickups. We demonstrated the results of efficient suppression of these effects by surface polynomials, calculated by combining EM simulations with 2D fitting. This methodology has great potential to be applied for any BPM of a modern accelerator.

However, testing these polynomials with actual real-time beam orbit monitoring is a challenge because it is difficult to produce large amplitude orbits. For historical (and simplicity) reasons the calibration of 1100 LHC BPMs before 2013 was limited to a 5th-order 1D polynomial, which was sufficient for most operational situations, except for several critical BPMs near the collision points. The correction of all LHC BPM families will be replaced by proper 2D polynomials after 2015. At the moment all 120 BPMs of ALBA are using linear BPM calibration with constant calibration factors. For studies of non-linear correction, the data will be analyzed off-line during upcoming machine studies.

REFERENCES

[1] CST Studio: http://www.cst.com

[2] A. A. Nosych and M. Wendt, "Analysis of Geometric Non-Linearities of LHC BPMs by 2D and 3D Electromagnetic Simulations", PRST-AB (to be published).

[3] ACE3P Suite: www-group.slac.stanford.edu/acd/

[4] R. W Helms. and G. H. Hoffstaetter, "Orbit and optics improvement by evaluating the nonlinear beam position monitor response in the Cornell Electron Storage Ring", Phys. Rev. ST Accel. Beams, vol. 8, issue 6, 2005.

[5] A. Olmos et al., "Matlab code for BPM button geometry computation", Proc. DIPAC 2007, pp. 186-188, 2007.

[6] A. Stella, "Analysis of DAΦNE BPM with a boundary element method", DAΦNE Technical Note, INFN, 1997.

[7] A. A. Nosych, "Geometrical non-linearity correction procedure of LHC beam position monitors", EDMS doc. no. 1342295, CERN, 2014.